UNDERSTANDING AND PROCESSING OF THE FIELD EMISSION ENHANCED BY CONDUCTING PROTRUSIONS*

M. LUONG[a,†], H. SAFA[a], B. BONIN[a], T. JUNQUERA[b], A. LE GOFF[b] and S. MAÏSSA[b]

[a]*CEA-DAPNIA-SEA BP no 2, 91191 Gif sur Yvette Cedex, France;*
[b]*IPN (CNRS-IN2P3), 91406 Orsay Cedex, France*

In the last decades, several investigation on enhanced field emission from metallic surfaces pointed out the importance of intrinsic surface defects and particle contamination, as potential emitters. Today, chemical or electropolishing on the one hand and high pressure water rinsing on the other give very high performance single cell niobium cavity ($E_{acc} = 30-40\,\mathrm{MV\,m^{-1}}$). Nevertheless, it seems difficult to reach identical performances on nine cells cavities. Thus, a better understanding of the emitting and processing mechanisms of the most potential emitters: conducting protrusions, appears still useful. Our experimental results showed a high consistency with the explanation that field enhancement factor β, in the Fowler–Nordheim's law, came from a geometrical effect due to the superposition of nanometer size protrusions on micron size ones. A comparison of β and A_e – the effective emitting area – of the same emitter in DC and RF regime gave the same values. Furthermore, it was possible to check that a crater-like defect presented an emission on the rim, in both DC and RF regimes. According to the geometrical explanation, smoothing a protrusion should strongly reduce the emission. This prediction was verified by using a thermal and a mechanical treatment. At last, the *in situ* RF processing, called High Peak Power Processing, had been simulated on small samples, manufactured in different metals. The results had not indicated a significant dependence on the material properties, but pointed out the role of a high current density. A value near $10^{12}\,\mathrm{A\,m^{-2}}$ initiated a run away event that ended in the emitter explosion.

Keywords: Superconductivity; Radiofrequency; Cavities; Field emission

---

1. INTRODUCTION

Electron emission from a metallic surface submitted to a high electric field appeared long ago as an endemic problem for DC or RF devices operating at high voltage, because of the resulting leak current and breakdown risk. In accelerating RF cavities, especially in super-conducting ones, this field emission set up a severe and high cost limi-tation. It prevented from constructing short accelerator modules.

During the last decades, many experiments had been undertaken separately in DC and RF regime, either on small samples or on large surfaces as cavities. They identified potential emitters as being micro-scopic random contamination particles or surface defects, like scratches or inclusions. Experimental observations proved there should not be only a single mechanism responsible for enhanced field emission since the emitters could have insulator, semi-conductor or conductor prop-erties. An underlying physical mechanism had been proposed for each case: filament and hot electron explanation for insulators and semi-conductors,[1,2] superposed metallic protrusions for conductors.[3] Nevertheless, according to Maley[4] and Jimenez et al.,[5] it appeared that conducting contaminants caused stronger field emitted currents, with low field threshold, and made the contaminated devices more difficult to condition. For this reason, the conducting protrusions deserved an extended investigation.

2. EMISSION PROPERTIES IN DC AND RF REGIMES

An identity of the parameters (β and A_e), in DC and RF regimes, was expected from the superposed protrusions explanation, which was ultimately based on the Fowler–Nordheim theory. The parameter β was considered as the result of a geometrical effect that enhanced the applied field E. The local field on the top of the micrometric protrusion raised to $\beta_1 E$. If this protrusion supported a much smaller one (of tens nanometer size), the final local field raised to $\beta_2(\beta_1 E)$. A comparison of these parameters on the same emitter would deny or consolidate such an explanation.

A first comparison had been attempted by Tan,[6] on metallic particles, in our laboratory, and had given encouraging indications for identity,
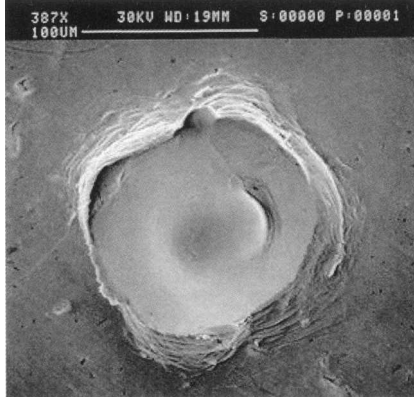
FIGURE 1   Crater-like emitter.

even though the DC current had been blurred by fluctuations. These fluctuations were found to be caused by adsorption.[7] With the help of a proper desorption, we renewed the comparison on crater-like emitters (Figure 1).

Each emitter was intentionally prepared on the very clean surface of a small sample. Its characteristics were typically of 100 μm in diameter and 10 μm in height. The field emission current was measured versus the applied field first at 1.5 GHz, and next at DC field, in two distinct apparatus (a re-entrant cavity and a SEM equipped for field emission study.[6] Afterward, emission parameters were estimated from experimental data and modified Fowler–Nordheim's formulae:

$$I_{DC}(E) = A_{eDC} \frac{1.54 \times 10^{-6} \beta_{DC}^2 E^2}{\phi} \exp\left(- \frac{6.83 \times 10^9 \phi^{1.5}}{\beta_{DC} E}\right), \quad (1)$$

$$\langle I_{RF}(E_{peak}) \rangle = A_{eRF} \frac{M \beta_{RF}^{2.5} E_{peak}^{2.5}}{\phi^{7/4}} \exp\left(- \frac{6.83 \times 10^9 \phi^{1.5}}{\beta_{RF} E_{peak}}\right). \quad (2)$$

Full details about experimental set-up and procedure can be found elsewhere.[8] Very close characteristics were obtained (Table I) provided that precautions were observed in order not to contaminate or modify physically the emitter between the RF and DC measurements.

TABLE I   Emitting characteristics in DC and RF regimes

	β_{RF}	β_{DC}	A_{eRF} (m^2)	A_{eDC} (m^2)
Copper	274	260	2.3×10^{-16}	4.8×10^{-16}
Niobium	222	214	10^{-16}	1.7×10^{-16}
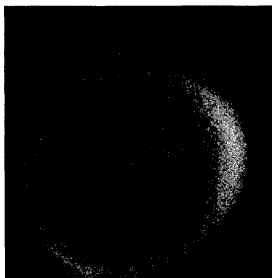
FIGURE 2   Electronic pattern from a crater-like emitter in RF regime.
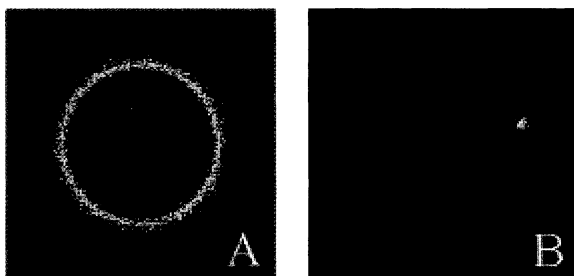

FIGURE 3   Simulated patterns with: (A) uniform distribution of pin-point sources on the rim, (B) single source.

In the DC regime, probing a crater-like with a small anode tip of a few microns radius curvature, in our SEM, had localized the electron sources on the crater rim. To check the same kind of distribution in the RF regime, an electronic pattern of the beam was obtained by focusing electrons with a magnetic lens on a phosphorescent screen.[9] Experimental patterns like that shown in Figure 2 suggested a similar distribution.

Thanks to the electric and magnetic field maps given by a numerical code (URMEL), the electrons trajectories could be tracked, and simulated patterns obtained with specific electron source distributions on the rim (Figure 3). Clearly, the field emission current in RF regime

also came from the protuberant rim of an emitter. The identity of the emitting characteristics and electron source localization, in both DC and RF regimes, proved consistent the geometrical explanation for the enhanced emission.

3. THERMAL AND MECHANICAL SURFACE TREATMENTS

One important consequence of the superposed protrusions explanation would be: a superficial damage of an emitter, by means of thermal or mechanical strain, should lead to a strong reduction of the undesired emission. There would be no need to remove completely a protrusion. This opened some new perspectives to fast, economical and easy treatments that we investigated.

3.1. Electron Beam Surface Heating

The idea consisted in melting superficially the protrusions using an intense electron beam provided by a electron welding apparatus. The treatments happened under secondary vacuum (10^{-4} Pa), thus preventing the surface from significant oxidizing. There were four critical beam parameters: voltage, current, diameter, and sweep frequencies. The voltage fixed the penetration depth, which also depended on the material density. For molybdenum and niobium, whose density is respectively 1.02×10^4 and 8.4×10^3 kg m^{-3}, a 25 kV beam dissipates in 1.5 µm. To produce a superficial melting on protrusions and not on the entire surface, the beam had to deposit locally a high power density in a short time. A thermal conduction model gave an estimation for the remaining key values.[9] The beam diameter was chosen as 0.5 mm, the current 0.1 A, the highest sweep frequency 1000 Hz and the lowest 10 Hz (Figure 4). With this configuration, each point of the surface was exposed to a power density of 1.3×10^{10} W m^{-2} during 5 µs every 0.1 s.

3.1.1. Molybdenum Samples

A small surface less than 1 mm^2, mechanically polished with ⊘ 0.1 µm alumina paste, then carefully rinsed with ultra-pure water, was generally emission free, or at least emitted a low current (< 0.1 µA) up to
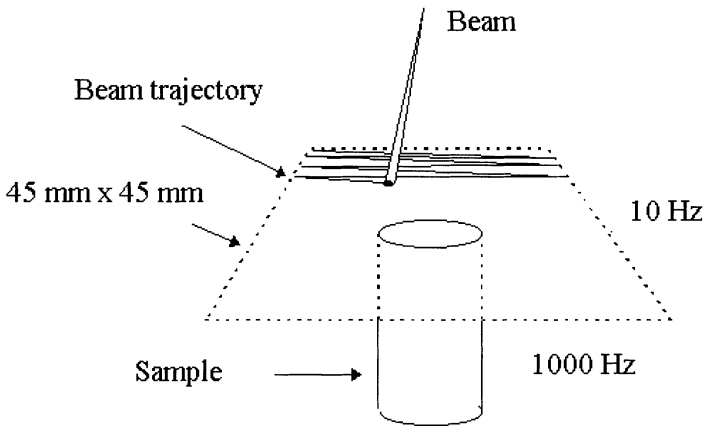
FIGURE 4   Electron beam treatment configuration.

$100 \, MV \, m^{-1}$. To evidence the treatment benefit, emitters were added to the surface by touching it slightly with a tungsten tip. The sample was first tested in the 1.5 GHz re-entrant cavity, then treated by the electron bombardment during 10 and 1 s respectively for sample Mo1 and Mo2. Next, the sample was rinsed and tested again. At last, the emitted current, before and after the treatment was compared (Figure 5).

The treatment produced an important current reduction. It only remained to check that there were no strong physical modifications but superficial ones on the emitters. This was realized by comparing the pictures of emitters, taken in the SEM, before and after the treatment (Figure 6), that confirmed no visible change down to micron scale. A 10 s treatment appeared more effective than its 1 s equivalent. The explanation lay on a cumulative effect that raised the bulk temperature of the sample from one sweep to another. Insofar as the maximum temperature, reached on the top of a protrusion in a sweep, depends on the geometry and the sample initial temperature, a longer treatment favored a superficial melting.

3.1.2. Niobium Samples

To generalize these results, four niobium samples underwent the same treatment. Their surfaces were made very rough (Figure 7) in purpose,
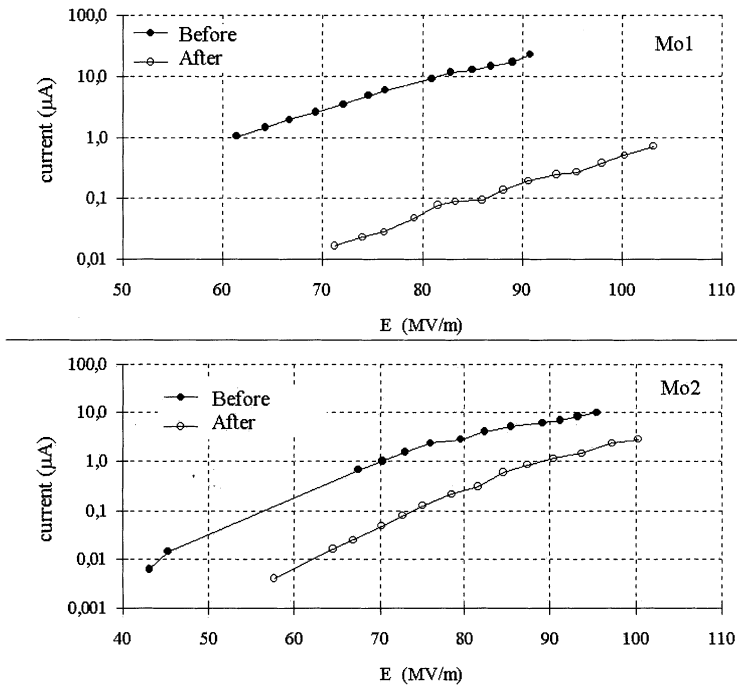
FIGURE 5   Surface heat treatment benefit on emission reduction.

by grinding and scratching them, in order to test more severely the effectiveness of this kind of treatment.

Currents were measured at $40\,\mathrm{MV\,m^{-1}}$ once again before and after a 10 s treatment (Figure 8). Conclusion was straightforward. All these results supported the explanation that protrusions on a micrometric protrusion played a critical role.

3.2. High Pressure Water Rinsing (HPWR)

This procedure consisted in directing a high pressure water jet, generally of 10 MPa, on the surface to be rinsed. It proved very effective to reduce field emission in superconducting cavities.[10] High performance single cell cavities were obtained with good reproducibility recently.[11]

The success of such treatment was attributed only to a dust removal; contamination particles were drift by the flow. Indeed, even at normal incidence, the mechanical strain created by a continuous jet on the
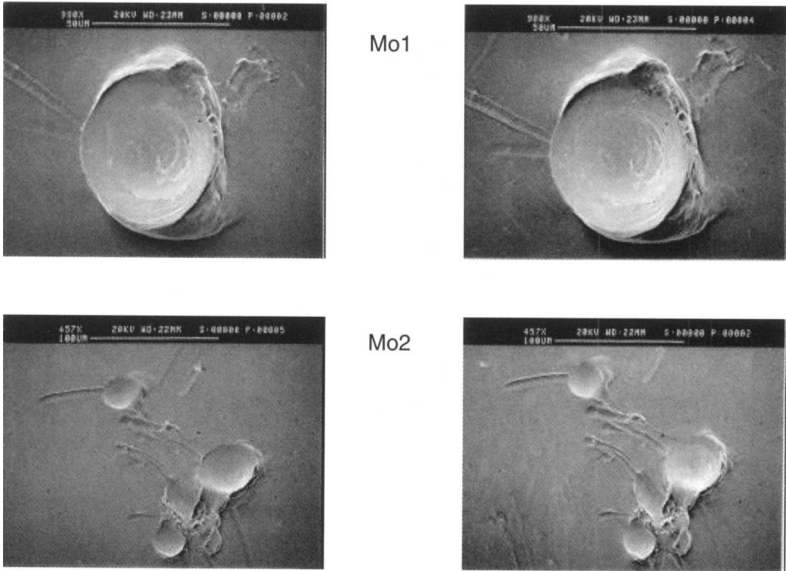
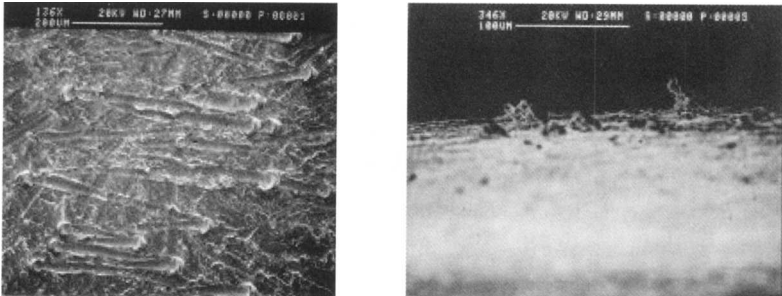FIGURE 6 SEM pictures of emitters before (left) and after (right) the treatment.

FIGURE 7 Top view (left) and side view (right) of a rough niobium surface.

surface would be much inferior to the tensile strength of niobium (~ 200 MPa). With a pressure of 10 MPa, the pumping group delivered 10 l of water per minute through two 0.8 mm diameter orifices in the nozzle. This corresponded to a jet velocity of 166 m s^{-1}, giving a strain of 14 MPa ($\rho v^2/2$ where ρ is the water density).
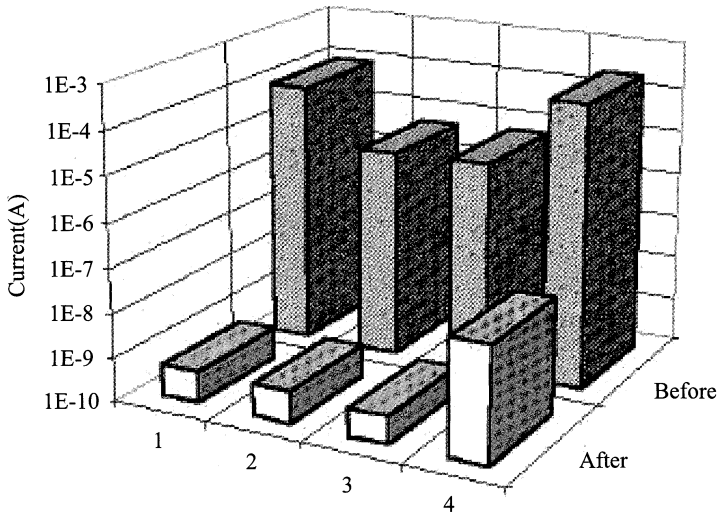
FIGURE 8   RF emission current at $40\,\mathrm{MV\,m^{-1}}$, before and after a surface heat treatment, on four niobium samples.

However, the continuous jet should be surrounded by a sheath of droplets drift with a velocity near that of the core. The impacts of such droplets are amplified by a shock wave effect,[12] known as "hammering effect". The resulting mechanical strain can overreach $250\,\mathrm{MPa}$ ($\rho u v$, where u is the sound velocity in water). From this analysis, it was allowed to expect some erosion effect or a more noticeable modification on intrinsic protuberant defects.

To check the predictable effect, the morphology of emitters on four niobium samples had been examined in a SEM before and after HPWR (Figures 9–12). The rinsing apparatus was similar to it equivalent at CEBAF,[10] with the difference, nevertheless, that our nozzle included only two orifices instead of eighteen. Pressure and delivery took the values in the previous analysis. The surfaces under study were placed at a distance from the nozzles, equal to the iris radius of a $1.3\,\mathrm{GHz}$ cavity. They went twice (up and down) past of the nozzle, animated with a circular movement of one lap every $3\,\mathrm{s}$, as a surface of a cavity under rinsing would. Before the treatment, surfaces emitted currents around $1\,\mathrm{\mu A}$ at $40\,\mathrm{MV\,m^{-1}}$. These currents fell down to $1\,\mathrm{nA}$, the detection

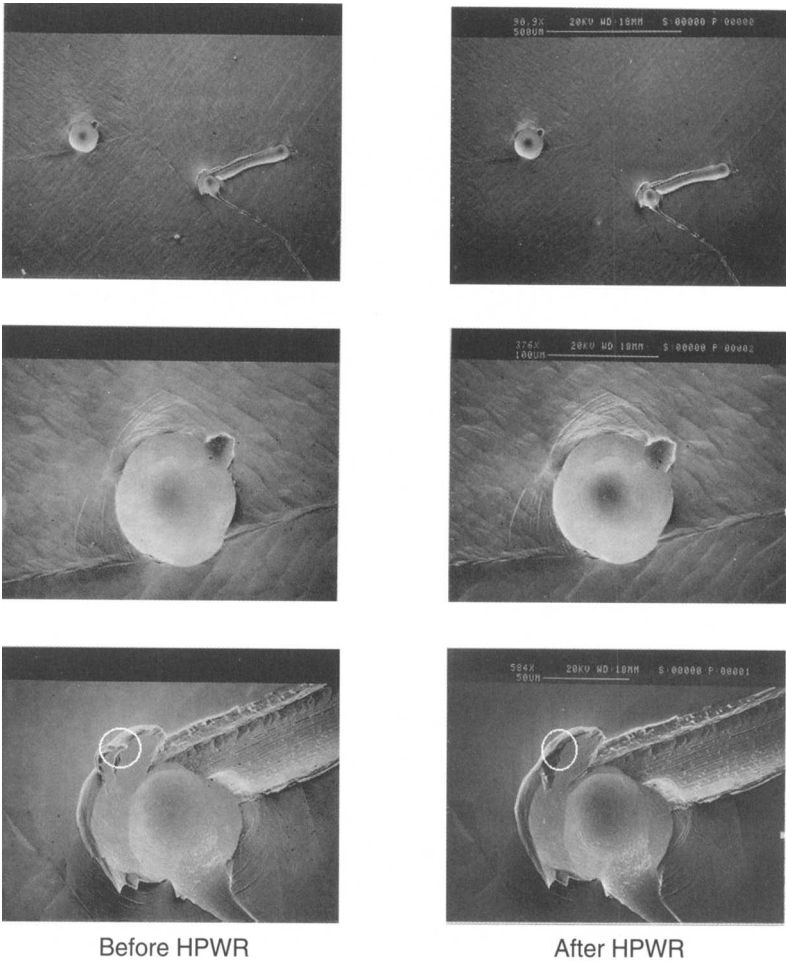Before HPWR   After HPWR

FIGURE 9   Emitter morphology change during HPWR on sample Nb1.

threshold being 0.1 nA. This result was common to every surface whose emitters underwent more or less noticeable modifications.

As a conclusion, this experiment pointed out a stronger mechanical effect of HPWR on a niobium surface, in addition to a dust removal. This effect originates in the structure of a real high pressure jet, which can be controlled by optimizing the nozzle geometry.
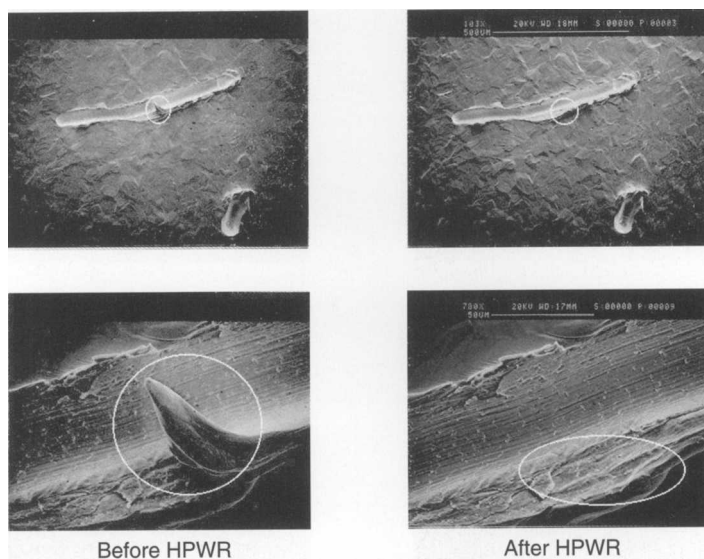
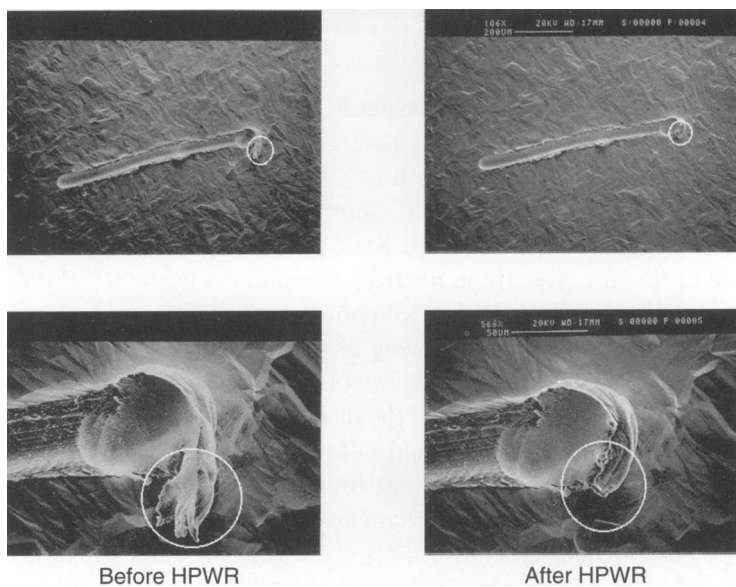FIGURE 10   Emitter morphology change during HPWR on sample Nb2.

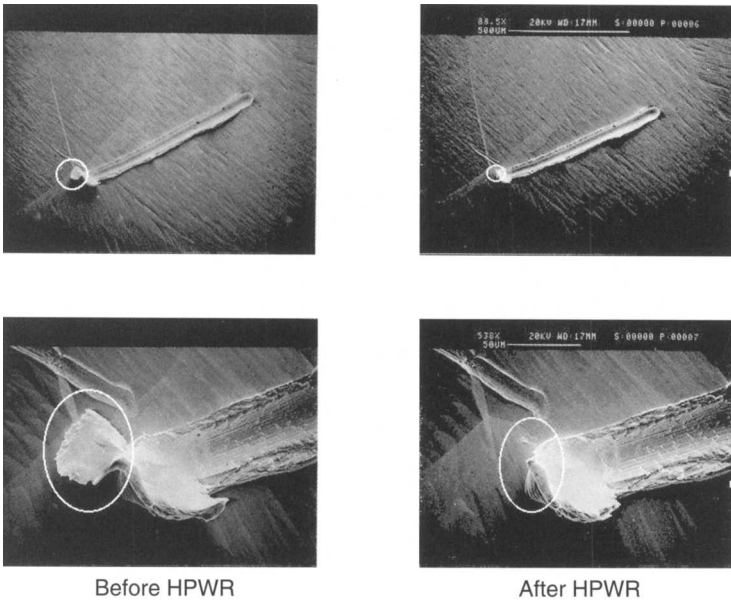FIGURE 11   Emitter morphology change during HPWR on sample Nb3.

Before HPWR   After HPWR

FIGURE 12   Emitter morphology change during HPWR on sample Nb4.

4. *IN SITU* RF PROCESSING

The *in situ* RF processing often remains the treatment as the last resort, when a cavity is subjected to field emission, once mounted in its operational environment. It consists of applying repetitively a high electric field on a surface during a short time; i.e. feeding a cavity with high power pulses. Such a high peak power processing (HPPP) had proved generally effective in the field emission eradication.[13,14] Nevertheless, a few failures had also been observed. Studies were going on in order to get a better understanding of the processing mechanism, and infer a more reproducible procedure. In our laboratory, we had already investigated a possible impact of the thermal and mechanical properties (melting point and tensile strength) of the metal that composed a protrusion.[15] The experiment had not found any linear relation between these properties and the final characteristics (β, A_e), but had brought out a current density limit ($10^{12}\,A\,m^{-2}$) beyond which a run away phenomenon was initiated. This current density limitation allowed a prediction of the processing effectiveness in terms of field enhancement
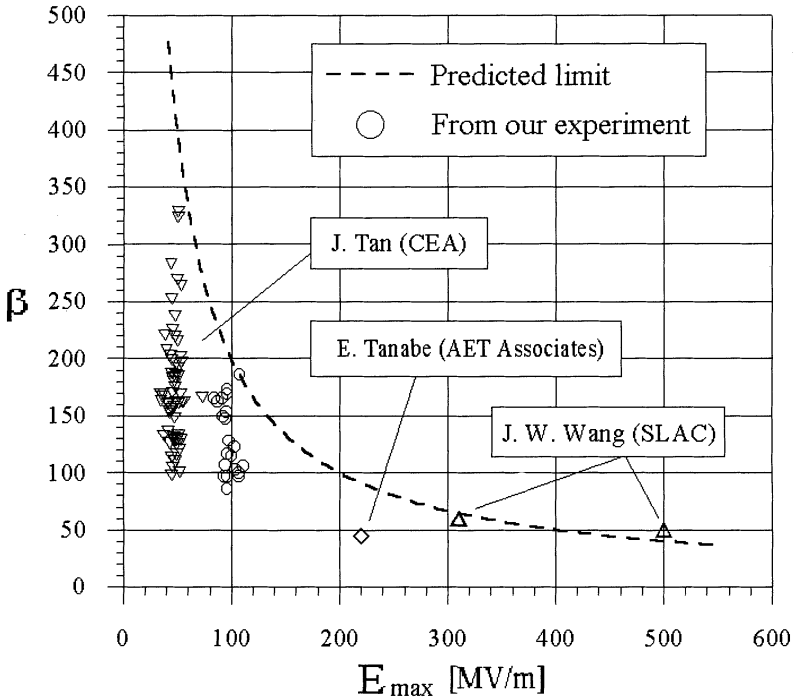
FIGURE 13   Field enhancement factor after a RF processing, compared to the prediction based on the high current density limitation (10^{12} A m^{-2}).

factor. Using Eq. (2), it was possible to compute the maximum value of β for the dominant emitter on a surface processed at a given field E_{max}. The prediction was compared to several experimental results: Tan's,[16] Wang's,[17] Tanabe's[18] and ours (Figure 13).

This picture indicate the good correlation between prediction and experiment, hence the importance of the current density limit. It also stresses on how worthy a processing at $200 \, MV \, m^{-1}$ could be, for a surface that have to sustain a nominal $50 \, MV \, m^{-1}$.

A processed surface showed evidences of molten craters. Their diameter ranked at a few microns (Figure 14). Creation of molten crater were thought to be related to important sudden current drops observed as the fields were raising during the processing.

In a recent experiment, we monitored the current signal and luminous emission signal. The samples were processed in a cavity equipped with
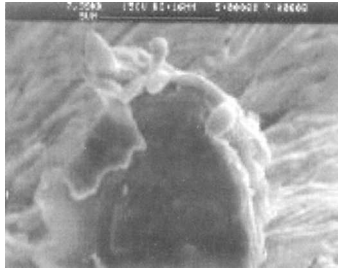
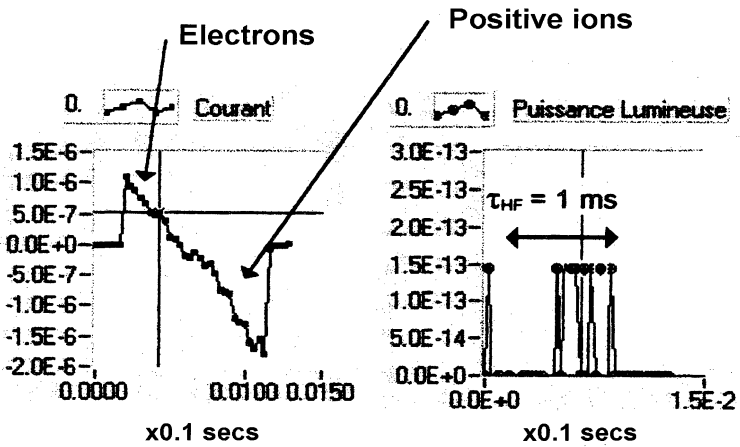FIGURE 14 Trace of molten crater on a processed surface.

FIGURE 15 Positive ion burst (left) and luminous spot (right) associated with a processing event on a copper sample.

an optical line.[19] This allowed to correlate both the signals inside a macro-pulse (1 ms) and from a pulse to another. Generally, a processing event was preceded by weak current fluctuations that quickly ended in a current inversion, i.e. burst of positive ions. The inversion began in the middle of a macro-pulse; at the time, a luminous emission was detected (Figure 15).

Very short (few nanoseconds) luminous spot had been reported on DC cathodes.[20] Here, the much longer spot rather suggested a

thermal emission by a small pool of molten copper. This emission would have a spread spectrum. Knowing the pass band (180–850 nm) of the photo-amplifier, the detection solid angle ($\Omega = 2.5 \times 10^{-3}$ steradian) and transmission efficiency ($\eta = 0.6$) of the optical line, it was possible to estimate the measured power. Let us consider a molten copper pool ($\oslash$ 5 µm) of area A_f, at a temperature of 1356 K, emitting in a hemisphere as a gray body. At that temperature, the emissivity ε_T would be 0.16. Then the power is:

$$P = \eta \frac{\Omega}{2\pi} A_f \varepsilon_T \int_{180-850nm} \pi L_\lambda^0 \, d\lambda, \qquad (3)$$

where L_λ^0 represented the black body luminance. This gave $P = 1.3 \times 10^{-13}$ W, which was close to the measured value.

Finally, we have evidenced the part played by a high current density, confirmed the generation of a micro-plasma in processing events, and got an insight into their dynamics. Computational studies on micro-plasma ignition and growing are being undertaken by Padamsee and Knobloch at Cornell University.

5. CONCLUSION

These experimental studies proved the consistency of the superposed protrusions as explanation for the most dangerous emitters, the conducting protrusions. The idea of wearing out the protrusions to suppress the enhanced field emission had operated successfully. By extension, every process that could smooth a surface without contaminating it would be effective. Simulations of *in situ* RF processing on samples provided several practical indications on its mechanism and limitation. Nevertheless, they did not lead to a guideline for the best operational scenario, if ever this could exist. As a matter of fact, the geometry of a protrusion must play a significant part in how the current density reaches its limit value. On a real surface, emitters do have a random geometry. As a prospective statement for high gradient accelerating cavities, the finding of a non-contaminating assembling method will remain the major challenge, while high pressure rinsing effectiveness can be improved.

References

[1] Dearlnaley, G. (1969) *Thin Solid Film*, **3**, 161–174.

[2] Bayliss, K.H. and Latham, R.V. (1986) *Proc. Roy. Lond. A.*, **403**, 285–311.

[3] Jimenez, M., Noer, R.J., Jouve, G., Jodet, J. and Bonin, B. (1994) *J. Phys. D: Appl. Phys.*, **27**, 1038–1045.

[4] Maley, J.J. (1974) *J. Vac. Sci. Technol.*, **11**(5) 892–895.

[5] Jimenez, M., Noer, R.J., Jouve, G., Jodet, J. and Bonin, B. (1993) *J. Phys. D: Appl. Phys.*, **26**, 1503–1509.

[6] Tan, J. (1995) *Proceedings of the Seventh Workshop on RF Superconductivity (Gif sur Yvette)*, Vol. I, pp. 105–117.

[7] Luong, M. *et al.* (1995) *Proceedings of the Seventh Workshop on RF Superconductivity (Gif sur Yvette)*, Vol. II, pp. 509–511.

[8] Luong, M. *et al.* (1997) *J. Phys. D: Appl. Phys.*, **30**, 1248–1251.

[9] Luong, M. (1997) Ph. D. Dissertation, Pierre et Marie Curie University (Paris).

[10] Kneisel, P. and Lewis, B. (1995) *Proceedings of the Seventh Workshop on RF Superconductivity (Gif sur Yvette)*, Vol. I, pp. 311–327.

[11] Ono, M. *et al.* (1997) *Proceedings of the Seventh Workshop on RF Superconductivity (Abano)* (to be published).

[12] Spain, I.L. and Paauwe, J. (1977) *High Pressure Technology*, Vol. II, Marcel Dekker, pp. 465–479.

[13] Kirchgessner, J. *et al.* (1993) *Proceedings of the 1993 Particles Accelerator Conference*, Vol. 2, pp. 918–920.

[14] Graber, J. *et al.* (1994) *Nucl. Instr. and Meth. in Phys. Res. A*, **350**, 582–594.

[15] Luong, M. *et al.* (1995) *Proceedings of the Seventh Workshop on RF Superconductivity (Gif sur Yvette)*, Vol. II, pp. 519–522.

[16] Tan, J. (1995) Ph. D. Dissertation, Pierre et Marie Curie University (Paris).

[17] Wang, J.W. (1992) *Linear Accelerator Conference Proceedings*, Vol. II, pp. 716–718.

[18] Tanabe, E. (1994) *Appl. Surf. Sci.*, **76/77**, 16–20.

[19] Maïssa, S. *et al.* (1994) *Proc. of EPAC 94*, Vol. 3, p. 2203.

[20] Jüttner, B. (1987) *IEEE Trans. Plasma Sci.*, **PS-15**(5), 474–480.